

Hybrid manufacturing of collector coins with free-moving features

*Pedro M.S. Rosado*¹, *Rui F.V. Sampaio*¹, *João P.M. Pragana*^{1*}, *Ivo M.F. Bragança*², *Carlos M.A. Silva*¹, and *Paulo A.F. Martins*¹

¹IDMEC, Instituto Superior Técnico, Universidade de Lisboa, Portugal

²CIMOSM, Instituto Superior de Engenharia de Lisboa, Instituto Politécnico de Lisboa, Portugal

Abstract. This paper presents a feasibility study on the use of hybrid manufacturing to fabricate collector coins with free-moving features. The approach begins with the fabrication of the different coin elements through blanking and additive manufacturing and ends with minting to connect these elements and impart lettering and reliefs on both coin surfaces. Two different concepts are introduced and analyzed based on the geometric and operative parameters of coin minting. Experiments and finite element computer simulations allow establishing the applicability window of the proposed coin concepts. These results, combined with those obtained from destructive tests, are then used to optimize the operative parameters concerning the final geometry and structural integrity of the coins. The feasibility of the new hybrid manufacturing approach is demonstrated through the fabrication of prototype coins with free-moving features.

1 Introduction

Collector coins are characterized by their quality, legal tenderness, and unique designs, commemorating historical, social, and cultural events that appeal to both collectors and investors. They differ from regular circulating coins due to (i) limited production quantities, (ii) the use of precious metals such as silver, gold, and platinum, and (iii) stringent design requirements, often featuring intricate engravings and finishes. From a manufacturing standpoint, minting collector coins is one of the most challenging metal forming processes due to the exceptionally high pressures on tooling required to produce the aforementioned complex shapes with extremely small and accurate details. Moreover, the complexity of collector coins is currently increasing as mints compete with each other in the global numismatic market to introduce innovative, disruptive, and technologically bold products [1].

Recent manufacturing trends of collector coins include the use of new materials, the design and fabrication of coins with non-conventional geometries, and the incorporation of joining by forming techniques to assemble different types of materials. These trends pose new challenges to mints because collector coins can no longer be manufactured through conventional routes involving rolling, blanking, rimming, polishing, and coin minting. Nowadays, their manufacturing processes must also address the challenges arising from

* Corresponding author: joao.pragana@tecnico.ulisboa.pt

increased geometric complexity, required accuracy, and the necessity of assembling different types of materials such as metals, polymers, and ceramics. These requirements are no longer compatible with traditional trial-and-error development of collector coins and tooling. They demand the use of finite element computer programs capable of creating digital twins to replicate collector coin minting, regardless of the complexity of the dies and collar, and regardless of the differences in materials of the disk blanks [2].

In recent years, the authors have been engaged in addressing some of the above-mentioned challenges through the development and utilization of a hybrid additive manufacturing route to fabricate collector coins. This route combines metal additive manufacturing, wire electro-discharge machining, polishing, and coin minting to produce collector coins with complex, customized, and intricately contoured holes that are not easily achievable through conventional coin minting [3]. The validity and reliability of the hybrid manufacturing route were primarily investigated through the fabrication of stainless-steel coin prototypes. Subsequently, it was applied in the industrial production of silver collector coins belonging to the 2023 numismatic plan of the Portuguese Mint. Finite element digital twins supported both developments and aided in redesigning the dies and the additive manufactured coin blanks to meet the intended high-quality standards for the collector coins.

These results demonstrate that hybrid manufacturing is a valid and reliable alternative route for translating innovative designs into high-value collector coins. The purpose of this paper is to further explore the potential of hybrid manufacturing of collector coins by extending its applicability to the fabrication of coins with free-moving features. The goal is to investigate how additive manufacturing and minting can be effectively combined for connecting specially designed elements with free motion features to the outer coin rings.

2 Materials and methods

2.1 Hybrid manufacturing

The extended hybrid manufacturing route for fabricating collector coins with free-moving features utilizes different materials and involves a three-stage sequence. Firstly, the outer coin ring made from an UNS C36000 copper alloy (free-cutting brass) is blanked out of a pre-rolled strip of the specified material and thickness.

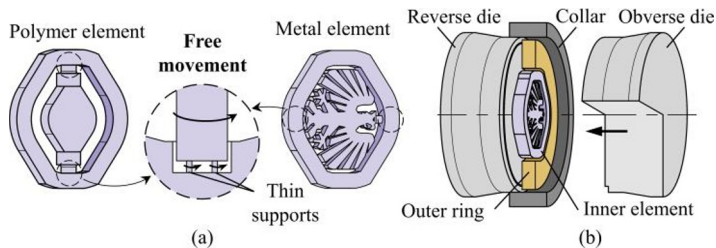


Fig.1. (a) Polymer and metal elements with free-moving features, and (b) minting with connection of the outer ring to the inner element with free-moving features.

Secondly, the inner elements with free-moving features are constructed by additive manufacturing, with thin supports incorporated during construction. The polymer elements are made from PLA (polylactic acid) and constructed by fused deposition modelling (FDM) whereas the metal elements are made from AISI 316L stainless steel and constructed by laser powder bed fusion (LPBF). The supports are subsequently twisted to release the element core and enable its free movement (Fig.1a).

Thirdly, coin minting is conducted to achieve two primary objectives: (i) connect the outer ring and inner element by means of a permanent force-fit joint, and (ii) impart lettering

and reliefs on both coin surfaces. This final stage of the extended hybrid manufacturing route is carried out using a press-tool system equipped with three main active tool parts: reverse and obverse dies, and a collar (refer to Fig.1b).

2.2 Mechanical characterization of the materials

The flow curves of the UNS C36000 copper alloy outer rings (Fig.2a), the AISI 316L stainless steel elements (Fig.2b) and the PLA elements with and without free-moving features (Fig.2c) were determined by compression and stack compression tests in accordance with the ASTM E9 standards. The results of these tests are included in Fig.2d. Since PLA is primarily subjected to compressive stresses, its tensile stress response was not considered relevant to determine, despite the variations in tension and compression behaviour commonly observed in polymers at ambient temperature (the so-called ‘strength-differential effect’).

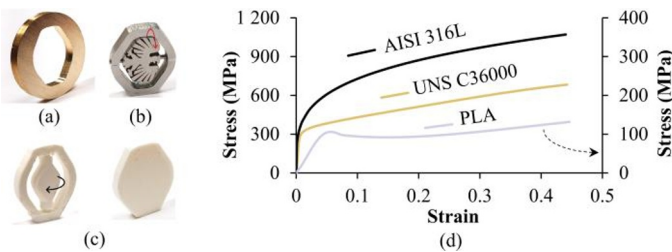


Fig.2. (a) Outer ring and inner elements constructed by (b) LPBF and (c) FDM. The flow curves of the materials are presented in (d) with the results of PLA displayed on the right-hand side axis.

2.3 Work plan

The connection of the outer ring to the inner element via a permanent force-fit joint was examined using outer rings with an inner hexagonal contour and inner elements without free-moving features, as depicted in Figs. 2a and 2c (right-hand side). As summarized in Table 1, the geometry of the inner elements remained constant, while that of the outer rings varied to accommodate different clearances (*i*). These clearances, along with the maximum coin minting force (F_{max}), constituted the primary parameters investigated in the work plan.

The effectiveness of the connection between the outer ring and inner element was assessed through destructive tests conducted in a universal testing machine, involving pushing the inner center out of the outer ring.

Table 1. Summary of the experimental conditions used in the work plan.

Coin elements		Dies	
Clearance <i>i</i> (mm)	Coin minting force F_{max} (kN)	Depth: (mm)	
0.1, 0.15, 0.2, 0.25	200, 250, 300, 350	<ul style="list-style-type: none"> □ 0 □ 0.08 ■ 0.12 ■ 0.15 ■ 1.00 	

The results of the primary parameter investigation and destructive testing were then utilized to fabricate the prototype collector coins with free-moving features, incorporating the inner elements depicted in Figs. 2b and 2c (left-hand side).

Regarding the tooling system, the dies were constructed from AISI D3 cold work steel and heat treated through hardening and tempering to achieve a hardness of 60 HRC. Additionally, the collar was fabricated from tungsten carbide with an inner diameter of 27.65 mm (refer to Table 1 for details).

2.4 Finite element modelling

Finite element modelling with the in-house finite element computer program i-form enabled the creation of digital twins of the coin minting stage of the hybrid manufacturing route [4]. The active tool parts (dies and collar) were modelled as rigid objects and discretized with contact-friction spatial triangles of constant friction ($m=0.2$). Outer rings and inner elements of the coins were assumed as deformable objects and discretized with hexahedral elements.

Two different strategies were employed. For inner elements without free-moving features, discretization utilized two symmetry planes to reduce the total number of elements to approximately 8000 hexahedra (Fig.3a). This preliminary set of simulations focused on investigating the mechanical contact between the outer rings and inner elements during coin minting. The use of symmetry planes reduced CPU time by approximately 8 times compared to simulations without symmetry. In the case of inner elements with free-moving features, symmetry planes were not employed, resulting in much larger meshes with approximately 60,000 hexahedra (Fig.3b). This increase in mesh complexity was necessary to analyze the impartation of lettering and reliefs on both coin surfaces during coin minting.

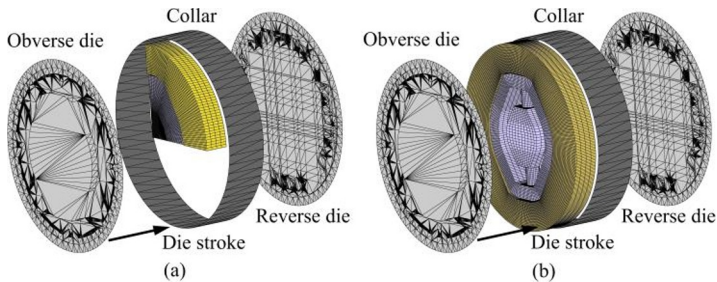


Fig.3. Finite element model of coin minting with inner elements: (a) without and (b) with free-moving features.

3 Results and Discussion

3.1 Material Flow

Coin minting tests with inner elements without free-moving features allowed identifying three different modes of deformation based on the clearance (i) and the maximum coin minting force (F_{max}) (see Fig.4). The first mode (Fig.4a) occurs when the clearance i is too high or the maximum coin minting force F_{max} is too low ($i = 0.1 \text{ mm}$, $F_{max} = 200 \text{ kN}$), resulting in the absence of force-fit locking between the outer ring and the inner element. In other words, the inner element remains loose after minting. The second mode (Fig.4b) is the most suitable for ensuring a good force-fit locking with appropriate plastic deformation of the inner element. The third mode ($i = 0.25 \text{ mm}$, $F_{max} = 350 \text{ kN}$), while also ensuring force-fit locking, results in excessive plastic deformation of the inner element, compromising its integrity and the overall coin design (Fig.4c).

These results are supported by finite element predictions of normal stresses along the Y and X axes. They demonstrate a lack of interface contact stresses in the left-hand side case (mode 1) and excessive contact stresses leading to significant deformation of the inner

element in the right-hand side case (mode 3). Under these circumstances, the process parameters ($i = 0.2 \text{ mm}$, $F_{max} = 300 \text{ kN}$) used in mode 2 were adopted for the experiments with inner elements featuring free-moving features.

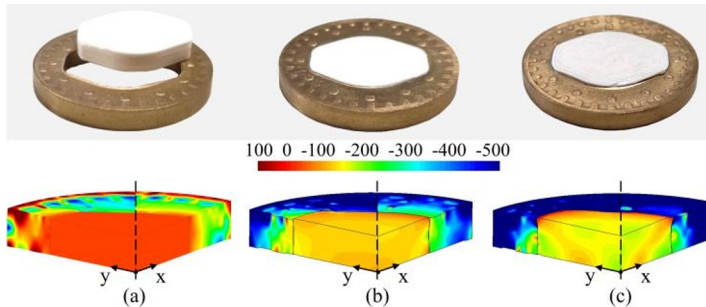


Fig.4. Coin samples with finite element predicted distributions of Y and X-stresses at the end of coin minting for (a) mode 1, (b) mode 2 and (c) mode 3. Note: The dashed vertical line separates the finite element predictions of Y-stress (left-side) and of X-stress (right side).

3.2 Forces

Fig.5a presents the experimental and finite element predicted force vs. die stroke evolution during coin minting of samples with process parameters corresponding to deformation mode 2 ($i = 0.2 \text{ mm}$, $F_{max} = 300 \text{ kN}$).

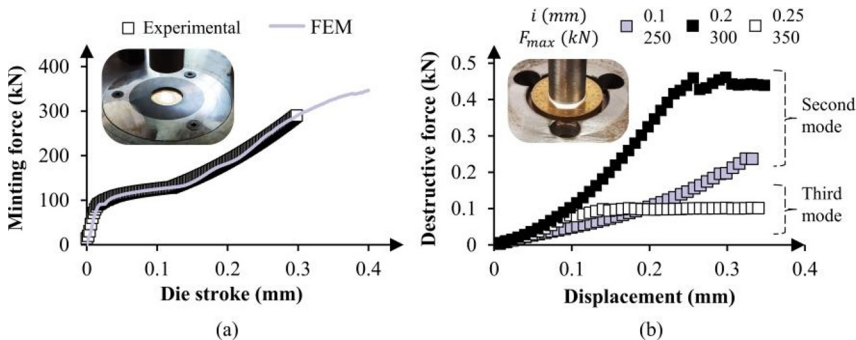


Fig.5. (a) Experimental and finite element predicted evolution of the coin minting force with die stroke ($i = 0.2 \text{ mm}$, $F_{max} = 300 \text{ kN}$) and (b) experimental evolution of the force with displacement for destructive tests performed with coin samples corresponding to deformation modes 2 and 3.

The evolution is characterized by a steep increase at the beginning due to the initial contact of the dies with the outer ring surfaces, followed by a monotonic increase of the force at a lower rate during impartation of lettering and reliefs on both coin surfaces. The final trend (beyond a die stroke of 0.3 mm) shows a further decrease in the force rate, which is attributed to buckling of the inner element caused by plastic instability (refer to Fig.4c). This last result allows concluding that monitoring the force evolution during coin minting can be utilized to prevent buckling, which leads to coin samples with geometric defects.

Fig.5b illustrates the experimental force versus displacement evolutions obtained from destructive tests conducted on coin samples that are representative of deformation modes 2 and 3. The results indicate that mode 2 provides stronger force-fit connections between the outer rings and the inner elements. Furthermore, by increasing the maximum coin minting force from 250 kN to 300 kN while maintaining deformation mode 2 (i.e., changing the clearance i from 0.1 to 0.2 mm), the coin connection becomes stronger, with 87% increase in the maximum force required to separate the outer ring from the inner element.

3.3 Prototype coins with free-moving features

Fig.6 depicts the finite element-predicted evolution of Z-stress on the obverse side of two prototype samples during coin minting. The results demonstrate a progressive increase in the compressive Z-stresses (pressure) towards very high values, reaching approximately 1200 MPa. This increase in pressure facilitates the impartation of engravings and finishes, as well as the locking of the outer ring with the inner element by force-fit closure. This is achieved without excessive deformation or buckling of the inner elements that could eventually compromise the free movement of the features, thanks to the use of process parameters selected from mode 2 ($i = 0.2 \text{ mm}$, $F_{max} = 300 \text{ kN}$).

The absence of pressure at the inner elements (indicated by red color values) is a deliberate design choice, as detailed in Table 1, aimed at preventing damage to the free-moving features. Real samples are included on the right-hand side of Fig.6 to visually demonstrate the feasibility of the proposed extension of hybrid manufacturing to fabricate collector coins with free-moving features.

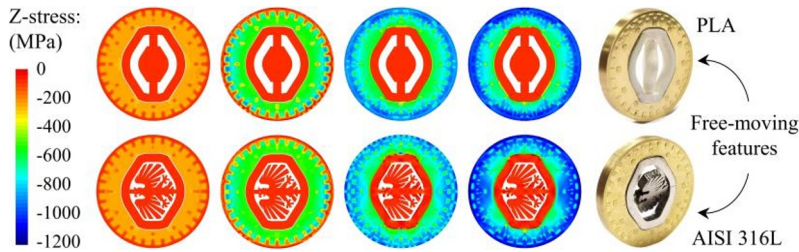


Fig.6. Finite element predictions of Z-stresses (pressure) at 15%, 50%, 85% and 100% of total die stroke for the coins with free-moving features constructed by additive manufacturing of PLA and of AISI 316 stainless steel. Photographs of the real prototypes are included in the right-hand side.

4 Conclusions

Extension of hybrid manufacturing routes combining blanking, additive manufacturing and coin minting was successfully employed to fabricate coins with free-moving features. Additive manufacturing was utilized to construct the inner elements with moving features, while coin minting applied the compressive pressure required to impart lettering and reliefs on the outer ring and obtain a force-fit locking between the two types of elements.

Results show that the quality of the coins is significantly influenced by the initial clearance (i) between the elements and the maximum coining force (F_{max}), leading to extreme situations where either the inner elements are loose or excessively deformed due to buckling. Finite element digital twins proved effective in replicating the coin minting process, estimating the forces, and enlightening the reasons behind the three different modes of deformation.

References

1. R. Grill, A. Gnadenberger, Int. J. Refract. Met. Hard Mater. **24**, 275 (2006).
2. J.P. Xu, Y.Q. Liu, S.Q. Li, S.C. Wu, Comput. Model. Eng. Sci. **38**, 201 (2008).
3. J.P.M. Pragana, S. Rosenthal, I.M.F. Bragança, C.M.A. Silva, A.E. Tekkaya, P.A.F. Martins, J. Manuf. Mater. Process. **4**, 115 (2020).
4. J.P.M. Pragana, S. Rosenthal, P. Alexandrino, A. Araújo, I.M.F. Bragança, C.M.A. Silva, P.J. Leitão, A.E. Tekkaya, P.A.F. Martins, Proc. Inst. Mech. Eng. B: J. Eng. Manuf. **235**, 819 (2021).